10.2478/msr-2014-0029
MEASUREMENT SCIENCE REVIEW, Volume 14, No. 4, 2014

Comparison of Molecular Iodine Spectral Properties at 514.7 and 532 nm Wavelengths

J. Hrabina[1], O. Acef[2], F. du Burck[3], N. Chiodo[2], Y. Candela[2], M. Sarbort[1], M. Hola[1], J. Lazar[1]

[1]Institute of Scientific Instruments, v.v.i., Academy of Sciences of the Czech Republic, Kralovopolska 147, 61264 Brno, Czech Republic, hrabina@isibrno.cz
[2]Sytèmes de Référence Temps Espace, SYRTE/LNE/Observatoire de Paris/UPMC, 61, avenue de l'Observatoire, 75014 Paris, France
[3]Laboratoire de Physique des Lasers, CNRS-UMR 7538, Universite Paris 13, Sorbonne Paris Cité, 99, avenue Jean-Baptiste Clément, Villetaneuse 93430, Paris, France

We present results of investigation and comparison of spectral properties of molecular iodine transitions in the spectral region of 514.7 nm that are suitable for laser frequency stabilization and metrology of length. Eight Doppler-broadened transitions that were not studied in detail before were investigated with the help of frequency doubled Yb-doped fiber laser, and three of the most promising lines were studied in detail with prospect of using them in frequency stabilization of new laser standards. The spectral properties of hyperfine components (linewidths, signal-to-noise ratio) were compared with transitions that are well known and traditionally used for stabilization of frequency doubled Nd:YAG laser at the 532 nm region with the same molecular iodine absorption. The external frequency doubling arrangement with waveguide crystal and the Yb-doped fiber laser is also briefly described together with the observed effect of laser aging.

Keywords: Laser spectroscopy, metrology, molecular iodine, absorption cells, frequency doubling, interferometry.

1. INTRODUCTION

MOLECULAR IODINE is one of the most common absorption media in laser spectroscopy and laser stabilization in the visible part of the optical frequency spectrum. It covers a spectral range from the green to near IR band and has a lot of very strong and narrow components, especially in the region close to the dissociation limit [1-4]. Molecular iodine is commonly used for frequency stabilization of lasers and it is also recommended by CIPM committee as an absorption medium for frequency stabilization of laser standards of length for different wavelengths [5]. Solid-state, frequency doubled Nd:YAG lasers stabilized by subdoppler saturation spectroscopy to hyperfine transitions in molecular iodine are used in metrological laboratories as stabilized lasers and represent the most stable optical references for interferometry and other applications in fundamental metrology. These lasers stabilized by saturation spectroscopy can achieve long-term frequency stability better than $1*10^{-14}$ for an integration time of 100 s, which means a more than two orders better result in comparison to traditionally used He-Ne-I_2 stabilized standards [6-16]. The short-term frequency noise of these lasers is also lower [17-20]. Further improvement in the short-term stability can be reached by means of prestabilization to a high-finesse passive optical cavity or by fiber based interferometer [21, 22]. Applications such as fundamental standards of length, optical frequency referencing of optical frequency combs, interferometry and also space applications dominate the field. Further, linear spectroscopy of molecular iodine is also an often used technique especially in case of interferometry applied at atmospheric conditions, where the influence of refractive index of air plays a dominant role [23-27]. Using this technique in combination with slow thermal tuning of the laser, the achievable frequency stability of frequency doubled Nd:YAG lasers is in the range of 10^{-9} for 100 s integration time which is often two orders better than refractive index caused noise [28-30]. However, excellent optical frequency stability achieved by these lasers stabilized to molecular iodine vapor by high resolution spectroscopy can be further improved. One of the possible approaches is to use modern fiber lasers that operate at wavelength closer to the dissociation limit of the molecular iodine, where narrower and even stronger absorption lines can be observed and used for laser stabilization [1-3, 31, 32]. Our goal was to investigate spectral properties of molecular iodine in the region of 514.7 nm with the help of frequency doubled Yb-doped DFB fiber laser and with a special interest to hyperfine components suitable for laser spectroscopy and laser standards stabilization purposes. These measurements follow the experiments done by J.-P. Wallerand et al., 6 years ago, with the same fiber laser which was handed over to the group of O. Acef several years ago. This laser was later equipped with a new arrangement for frequency doubling [32-34]. Laser aging produced a frequency shift of the laser optical frequency during this period. This effect resulted in an opportunity to scan another part of the iodine spectrum and to search for new interesting absorption lines. The spectroscopic measurement results were finally compared with those made at a 532 nm wavelength with the help of the same setup (including electronics) and the same absorption cells but with different frequency doubled Nd:YAG laser [1, 2, 5]. Special attention was devoted to the analysis of linewidths of the investigated hyperfine components at different environmental conditions.

2. EXPERIMENTAL SETUP

A. Laser head and Frequency doubling system.

The measurement at 514.7 nm wavelenght was performed with the help of frequency doubled Yb-doped DFB laser head with an external waveguide doubling crystal system. The laser itself delivers 12 mW near 1029 nm amplified up to 500 mW with a linewidth below 10 kHz level. The frequency tuning of the laser can be done through temperature control of the Bragg grating (BG) or by tuning of the ceramic piezoelectric actuator (PZT) which stresses the BG. The tuning range of the laser at IR is about 0.7 nm.

The second harmonic generation (SHG) is done by a MgO:PPLN waveguide crystal for CW doubling at 1029 nm wavelegnth in single pass configuration. The crystal was produced by the ion-exchange technique 2 μm below the surface of the crystal and was designed to SHG with a quasi-phase matching (QPM) temperature around 50°C. The input and output facets of the waveguide were AR coated at both 1030 nm and 515 nm. The numerical aperture (N.A.) of the waveguide was 0.16. We obtained an optical conversion efficiency of 17 % with the possibility to achieve a power of 33 mW of green from 197 mW of incident IR power, with a power coupling in the waveguide of 45 % [34, 35].

B. Molecular iodine absorption cells.

The experimental setup (described in the next section) uses two molecular iodine absorption cells prepared at the Institute of Scientific Instruments (ISI). These cells are made out of fused silica; they are both 500 mm long with optical windows of 32 mm in diameter (25 mm of useful aperture). The windows are equipped with AR coatings for 500-540 nm wavelength region and both absorption cells have a cold finger in the central part for control of the iodine vapor pressure. Thanks to the long history of absorption cell preparation technology at the ISI, we had measured the molecular iodine purity in these cells by the method of induced fluorescence and we had also measured the absolute frequency shifts several years ago [13, 16, 36]. Both cells show excellent molecular iodine purity and absolute frequency shifts of iodine stabilized Nd:YAG laser below the 1 kHz level. These results should ensure good preconditions for a hyperfine component linewidth measurement.

C. Experimental setup schematic.

The experiment was based on commonly used saturated absorption spectroscopy in molecular iodine and detection of the third derivative [37]. It can be divided into two parts. The first part is used for the laser frequency stabilization and the second part for the molecular iodine spectra scanning and recording. Schematic of the experimental setup is in Fig.1.

The first part of the arrangement with the Cell1 uses the third harmonic inline spectroscopy detection technique for the frequency stabilization of the laser to a selected molecular iodine hyperfine component [7, 10-12, 15]. This laser is equipped with a PZT for the tuning of the cavity length, which is used for modulation of its optical frequency. Sensitivity of the PZT tuning was 12.53 MHz/V (DFB laser) and 2.1 MHz/V (Nd:YAG laser), respectively.

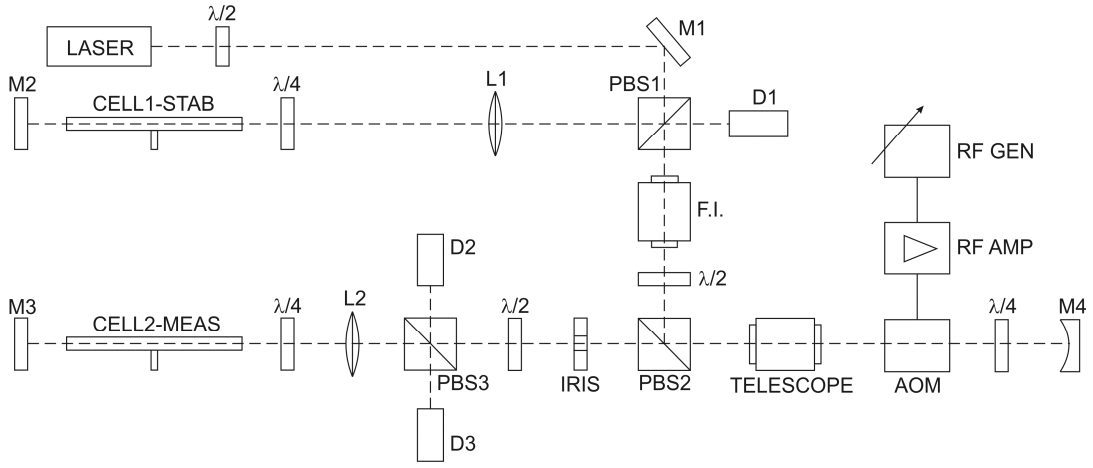

Fig.1. Experimental setup for the molecular iodine spectra measurement. Laser – Yb-doped frequency doubled DFB laser (λ=514 nm) or frequency doubled Nd:YAG laser (λ=532 nm), M1-M3 - full reflective dielectric mirrors, M4 – full reflective concave mirror (f=410 mm), PBS1-PBS3 – polarizing beam splitters, D1-D3 – photodetectors, F.I. – Faraday Isolator, L1-L2, Telescope – collimating optics, Cell1 – iodine absorption cell for the laser stabilization, Cell2 – iodine absorption cell for iodine spectra observation/scanning, AOM – acousto-optic modulator/ frequency shifter, RF Gen – signal generator, RF Amp – radio frequency amplifier.

The output beam from the laser is divided into two by polarizing beam splitter PBS1, first half of the optical power is used for saturation spectroscopy in molecular iodine in Cell1 and the signal for stabilization is detected by photodetector D1. Second part of the optical power from the laser beam comes out from PBS1 to Faraday Isolator F.I. before being collimated into the telescope to pass the AOM modulator/frequency shifter. The AOM is fed by a RF synthesizer followed by an amplifier to allow the precise control of the frequency shift of the optical frequency of the laser beam. The first-order diffracted beam passes through a λ/4 waveplate and is reflected back by the concave mirror M4 to PBS2 to achieve a double pass through the AOM resulting in a double frequency shift. A small portion of the

frequency shifted beam is used to monitor the laser power and AOM diffraction efficiency (D2). The rest is used to investigate the iodine profiles in Cell2 by saturation spectroscopy (D3). Scanning of the iodine spectra is done by frequency control of the AOM with the help of the PC controlled RF generator. Scanning of the hyperfine spectra of each Doppler broadened line is performed when the laser is locked to a selected iodine hyperfine transition with the help of the stabilization part of the experimental setup (Cell1) and recording of the iodine spectrum is done in the measuring cell (Cell2) over the whole tuning range of the AOM. The selection of this "stabilization transition" follows the need for scanning the part of the spectrum together with the available frequency shift of the AOM. Scanning over other hyperfine components needs relocking of the laser to another reference component. Measurement can be then repeated. A spectral recording over a larger spectral range is assembled from several frequency windows. We used two different freespace AOM frequency shifters, the first one with a tuning range of 200 ± 50 MHz and the second one with a tuning range of 110 ± 25 MHz. We were able to scan and record all observed lines and their hyperfine components with these two AOM shifters using +1 and -1 AOM diffraction orders (corresponding in double pass configuration to frequency shifts of 400 ± 100 MHz and 220 ± 50 MHz, respectively).

3. HYPERFINE COMPONENTS SPECTRA

At first the Doppler broadened molecular iodine spectrum at 514.7 nm wavelength was recorded over the temperature tuning range of the thermal shielded fiber laser. It was found that the laser aging effect had been probably caused by a slow, long-term creep of the dimensions of the laser/FBG which introduced a noticeable frequency shift of the output radiation at the level of ~0.17 nm/6 years (~28 pm/1 year). Thus, we were not able to reach the same absorption lines that were recorded 6 years ago with the same laser at the group of J.-P. Wallerand [32]. On the other hand this effect gave us a chance to investigate a new part of the iodine spectra and to find new perspective hyperfine components for laser frequency stabilization. We scanned 8 strong Doppler-broadened transitions within the available tuning range of the laser and we chose the three most promising ones – P46(44-0), P64(45-0) and R66(45-0) that seemed to have the best symmetrical profiles compared to the others within our frequency range. The spectral profiles of the hyperfine components from these lines were scanned. The most promising hyperfine component of each Doppler broadened line was studied in detail under different operating conditions to have an opportunity of comparison with molecular iodine spectral properties around the commonly used 532 nm wavelength.

The selection of the promising components was done with respect to their profile – its symmetry and linewidth. The a_{10} hyperfine component of the P46(44-0) absorption line was studied with a special care under different experimental conditions. This hyperfine component seems to perform the most promising shape and linewidth. An absence of other components in its neighborhood and its position at the center of the Doppler broadened profile seems to be the best and optimum choice for further metrological and laser frequency stabilization purposes. Influence of absorption media pressure, modulation width level and saturation intensity were investigated simultaneously together with the hyperfine component profile. We used a laser beam, diameter 1.5 mm, in both cases (514.7 and 532 nm wavelengths). The resulting measured linewidths under different experimental conditions were summarized in Table 1., Table 2. and Table 3., Fig.2., Fig.3. and Fig.4. together with the measurement of the well-known a_{10} component of the R56(32-0) absorption transition at 532 nm wavelength [5, 15, 16]. A sample record of one hyperfine component shows the signal-to-noise ratio achieved at 514.7 nm wavelength (Fig.5.). The errorbars in Fig.2.-Fig.4. express an overall estimated uncertainty (~15 kHz) caused mainly by the limited accuracy of the PZTs sensitivity calibration measurement (accuracy of modulation width evaluation) and AOM scanning resolution of the hyperfine spectra (10 kHz steps). The measurements were intended to be comparative, so a great care was taken to assure the same levels of all conditions and parameters (including using of the same optical setup/control and acquisition electronics). Identical levels of the intensity and diameter of the saturating beam at both wavelengths was achieved by using the same optical collimating optics and beam parameter measurement tools together with precise control of the beam power at the same time.

Table 1. Measurement of peak-to-peak widths (3f) of hyperfine components a_{10} P46(44-0) at 514.7 nm and a_{10} R56(32-0) at 532 nm wavelength - dependency on the modulation width (I_{sat}=2.3 mW/cm^2, T=-19.5°C (p=0.49 Pa)).

	λ=514.7 nm	λ=532 nm
	a_{10} P46(44-0)	a_{10} R56(32-0)
Δf_{mod} [MHz]	Δν [kHz]	Δν [kHz]
1.2	600	610
1.0	530	500
0.8	410	440
0.6	290	370
0.4	280	330

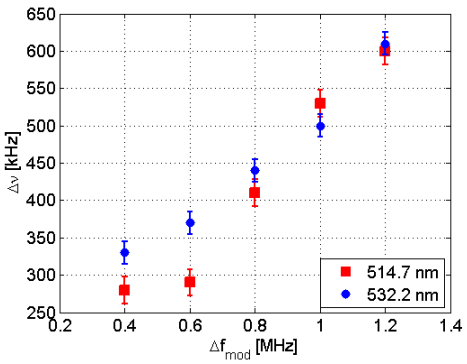

Fig.2. Measurement of peak-to-peak widths (3f) of hyperfine components a_{10} P46(44-0) at 514.7 nm and a_{10} R56(32-0) at 532 nm wavelength - dependency on the modulation width (I_{sat}=2.3 mW/cm^2, T=-19.5°C (p=0.49 Pa)).

The results of linewidth measurements of other promising hyperfine components of the P46(44-0), P64(45-0) and R66(45-0) lines at the limiting conditions are summarized in Table 4. It should be noted that the variation of linewidth between hyperfine components of the same rovibronic transition is due to predissociative effects. The natural width of hyperfine components is determined by the lifetime of hyperfine sublevels in the excited $^3\Pi_{0^+u}$ state which results, in addition to the radiative decay rate, in a predissociative decay rate due to the coupling with the $^1\Pi_{1u}$ dissociative state. In the absence of any magnetic field, this predissociative width is the sum of three terms corresponding to the gyroscopic predissociation, the hyperfine predissociation and the interference effect between both mechanisms [38-40]. As a result, the natural width of hyperfine components belonging to the same rovibronic transition can be significantly different from one component to another. This effect is particularly pronounced for low values of J for which the predissociative term is predominant [41].

Table 2. Measurement of peak-to-peak widths (3f) of hyperfine components a_{10} P46(44-0) at 514.7 nm and a_{10} R56(32-0) at 532 nm wavelength - dependency on the saturation intensity (Δf_{mod}=0.4 MHz, T=-19.5°C (p=0.49 Pa)).

		λ=514.7 nm	λ=532 nm
		a_{10} P46(44-0)	a_{10} R56(32-0)
P [μW]	I_{sat} [mW/cm^2]	Δν [kHz]	Δν [kHz]
40	2.3	280	330
61	3.4	280	330
81	4.6	290	340
107	6.1	300	340
150	8.5	300	370
250	14	315	380
400	23	320	380

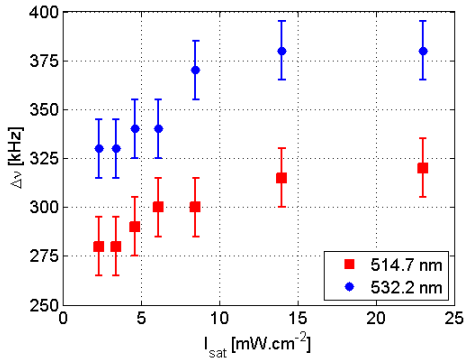

Fig.3. Measurement of peak-to-peak widths (3f) of hyperfine components a_{10} P46(44-0) at 514.7 nm and a_{10} R56(32-0) at 532 nm wavelength - dependency on the saturation intensity (Δf_{mod}=0.4 MHz, T=-19.5°C (p=0.49 Pa)).

Table 3. Measurement of peak-to-peak widths (3f) of hyperfine components a_{10} P46(44-0) at 514.7 nm and a_{10} R56(32-0) at 532 nm wavelength - dependency on the iodine pressure (I_{sat}=2.3 mW/cm^2, Δf_{mod}=0.4 MHz).

		λ=514.7 nm	λ=532 nm
		a_{10} P46(44-0)	a_{10} R56(32-0)
T [°C]	p [Pa]	Δν [kHz]	Δν [kHz]
-19.5	0.49	280	330
-15.0	0.83	310	350
-10.0	1.45	330	370
-5.0	2.48	370	380

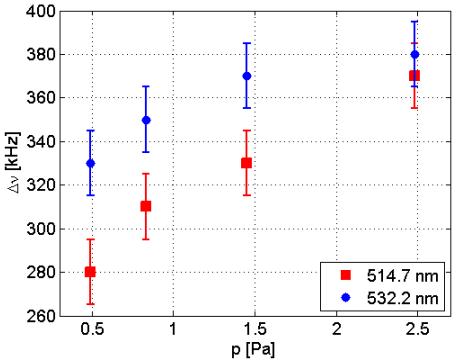

Fig.4. Measurement of peak-to-peak widths (3f) of hyperfine components a_{10} P46(44-0) at 514.7 nm and a_{10} R56(32-0) at 532 nm wavelength - dependency on the iodine pressure (I_{sat}=2.3 mW/cm^2, Δf_{mod}=0.4 MHz).

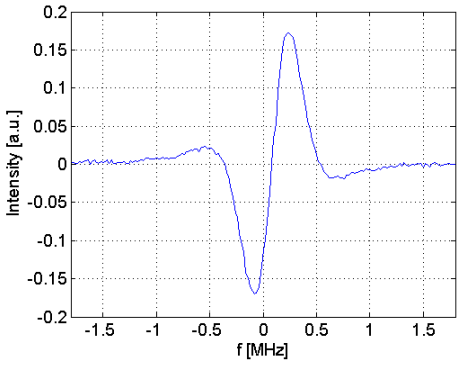

Fig.5. An example of achievable signal-to-noise ratio of 3f signal of hyperfine component a_{10} P46(44-0) at 514.7 nm (p=0.83 Pa, I_{sat}=8.5 mW/cm^2, Δf_{mod}=0.4 MHz).

Table 4. Measurement of the peak-to-peak widths (3f) of other promising hyperfine components of the P46(44-0), P64(45-0) and R66(45-0) absorption lines (I_{sat}=2.3 mW/cm^2, Δf_{mod}=0.4 MHz, T=-19.5°C (p=0.49 Pa)).

Line	Component	Δν [kHz]
P46(44-0)	a10	280
P46(44-0)	a6	310
P64(45-0)	a10	290
P64(45-0)	a15	300
R66(45-0)	a10	330
R66(45-0)	a15	350

4. DISCUSSION / CONCLUSIONS

We tried to use exactly the same conditions during the measurement at 514.7 and 532 nm wavelengths, respectively. The key result of this set of measurements is that the measured linewidths in 514.7 nm region are slightly narrower compared to the commonly used 532 nm wavelength. The narrowest linewidth (peak-to-peak width of third derivative) was measured for the a_{10} component of P46(44-0) line. The linewidth was 280 kHz (modulation width Δf_{mod}=400 kHz, absorption medium pressure p=0.49 Pa (T=-19.5°C) and saturation intensity level I_{sat}=2.3 mW/cm^2). The results of the measured linewidths of components from other neighboring lines were similar, close to the 300 kHz level. This confirms our expectation and means that this spectral region is of first interest for laser stabilization based on saturated absorption spectroscopy of molecular iodine with the opportunity to achieve better frequency stability. The very narrow transitions reflect also the excellent purity of the absorption media in the used iodine cells. In addition, the scanning technique used in this work has the potential to be a new method for detecting molecular iodine purity detection beside induced fluorescence and comparisons of frequency stabilized lasers on iodine. From Table 1., Table 2. and Table 3. above, it is evident that the main influence to the linewidth of the hyperfine profile has the level of modulation width of the modulation signal – its contribution to overall linewidth dominates above the 0.6 MHz levels. Intensity saturation starts to play a role at the level of about 7 mW/cm^2.

ACKNOWLEDGEMENT

The authors wish to express thanks for support to the grant projects from the Grant Agency of CR, project GPP102/11/P820, Academy of Sciences of CR, project: RVO:68081731, Ministry of Education, Youth and Sports of CR, projects: LO1212, CZ.1.05/2.1.00/01.0017, European Social Fund and National Budget of the Czech Republic, project: CZ.1.07/2.4.00/31.0016, the EMRP project IND58 6DoF and Technology Agency of CR, projects: TA02010711, TA0101995, TE01020233. The support of GRAM (CNRS-INSU) and of DGA/ANR (N°11 ASTR 001-01) is gratefully acknowledged by the French team.

REFERENCES

[1] Mironov, A.V., Privalov, V.E., Savelev, S.K. (1997). Complete calculated atlas of the absorption spectrum of iodine-127 (B-X system of bands) and complex of programs for the tabulation of iodine lines. *Optics and Spectroscopy*, 82 (3), 332-333.

[2] Salami, H., Ross, A.J. (2005). A molecular iodine atlas in ascii format. *Journal of Molecular Spectroscopy*, 233 (1), 157-159.

[3] Simmons, J.D., Hougen, J.T. (1977). Atlas of I2 spectrum from 19 000 to 18 000 Cm-1. *Journal of Research of the National Bureau of Standards, Section A : Physics and Chemistry*, 81 (1), 25-80.

[4] Cheng, W.Y., Chen, L.S., Yoon, T.H., Hall, J.L., Ye, J. (2002). Sub-Doppler molecular-iodine transitions near the dissociation limit (523-498 nm). *Optics Letters*, 27 (8), 571-573.

[5] Quinn, T.J. (2003). Practical realization of the definition of the metre, including recommended radiations of other optical frequency standards (2001). *Metrologia*, 40 (2), 103-133.

[6] Balhorn, R., Lebowsky, F., Kunzmann, H. (1972). Frequency stabilization of internal-mirror helium-neon lasers. *Applied Optics*, 11 (4), 742-744.

[7] Nevsky, A.Y., Holzwarth, R., Reichert, et al. (2001). Frequency comparison and absolute frequency measurement of I-2-stabilized lasers at 532 nm. *Optics Communications*, 192 (3-6), 263-272.

[8] Petru, F., Popela, B., Vesela, Z. (1993). Design and performance of compact iodine stabilized He-Ne lasers at lambda=633 nm with a short optical-resonator. *Measurement Science & Technology*, 4 (4), 506-512.

[9] Sevcik, R., Guttenova, J. (2007). Primary length standard adjustment. In *15th Czech-Polish-Slovak Conference on Wave and Quantum Aspects of Contemporary Optics*, Proc. SPIE 6609.

[10] Galzerano, G., Bava, E., Bisi, M., Bertinetto, F., Svelto, C. (1999). Frequency stabilization of frequency-doubled Nd : YAG lasers at 532 nm by frequency modulation spectroscopy technique. *IEEE Transactions on Instrumentation and Measurement*, 48 (2), 540-543.

[11] Nyholm, K., Merimaa, M., Ahola, T., Lassila, A. (2003). Frequency stabilization of a diode-pumped Nd:Yag laser at 532 nm to iodine by using third-harmonic technique. *IEEE Transactions on Instrumentation and Measurement*, 52 (2), 284-287.

[12] Bartl, J., Guttenova, J., Jacko, V., Sevcik, R. (2007). Circuits for optical frequency stabilization of metrological lasers. In *Measurement 2007 : 6th International Conference on Measurement.* Bratislava : Institute of Measurement Science SAS, 131-134.

[13] Hrabina, J., Petru, F., Jedlicka, P., Cip, O., Lazar, J. (2007). Purity of iodine cells and optical frequency shift of iodine-stabilized He-Ne lasers. *Optoelectronics and Advanced Materials-Rapid Communications*, 1 (5), 202-206.

[14] Ciddor, P.E., Duffy, R.M. (1983). Two-mode frequency-stabilized He-Ne (633 nm) lasers : Studies of short- and long-term stability. *Journal of Physics E : Scientific Instruments*, 16 (12), 1223-1227.

[15] Rovera, G.D., Ducos, F., Zondy, J.J., Acef, O., Wallerand, J.P., Knight, J.C., Russell, P.S. (2002). Absolute frequency measurement of an I-2 stabilized Nd : YAG optical frequency standard. *Measurement Science & Technology*, 13 (6), 918-922.

[16] Lazar, J., Hrabina, J., Jedlicka, P., Cip, O. (2009). Absolute frequency shifts of iodine cells for laser stabilization. *Metrologia*, 46 (5), 450-456.

[17] Hrabina, J., Lazar, J., Hola, M., Cip, O. (2013). Frequency noise properties of lasers for interferometry in nanometrology. *Sensors*, 13 (2), 2206-2219.

[18] Lance, A.L., Seal, W.D., Labaar, F. (1982). Phase noise measurement systems. *ISA Transactions*, 21 (4), 37-44.

[19] Hrabina, J., Lazar, J., Hola, M., Cip, O. (2013). Investigation of short-term amplitude and frequency fluctuations of lasers for interferometry. *Measurement Science Review*, 13 (2), 63-69.

[20] Rerucha, S., Buchta, Z., Sarbort, M., Lazar, J., Cip, O. (2012). Detection of interference phase by digital computation of quadrature signals in homodyne laser interferometry. *Sensors*, 12 (10), 14095-14112.

[21] Smid, R., Cip, O., Lazar, J. (2008). Precise length etalon controlled by stabilized frequency comb. *Measurement Science Review*, 8 (5), 114-117.

[22] Hodges, J.T., Layer, H.P., Miller, W.W., Scace, G.E. (2004). Frequency-stabilized single-mode cavity ring-down apparatus for high-resolution absorption spectroscopy. *Review of Scientific Instruments*, 75 (4), 849-863.

[23] Lazar, J., Hola, M., Cip, O., Cizek, M., Hrabina, J., Buchta, Z. (2012). Refractive index compensation in over-determined interferometric systems. *Sensors*, 12 (10), 14084-14094.

[24] Birch, K.P., Downs, M.J. (1994). Correction to the updated edlen equation for the refractive-index of air. *Metrologia*, 31 (4), 315-316.

[25] Lazar, J., Hola, M., Cip, O., Cizek, M., Hrabina, J., Buchta, Z. (2012). Displacement interferometry with stabilization of wavelength in air. *Optics Express*, 20 (25), 27830-27837.

[26] Lazar, J., Cip, O., Cizek, M., Hrabina, J., Buchta, Z. (2011). Standing wave interferometer with stabilization of wavelength on air. *tm-Technisches Messen*, 78 (11), 484-488.

[27] Zhang, J., Lu, Z.H., Menegozzi, B., Wang, L.J. (2006). Application of frequency combs in the measurement of the refractive index of air. *Review of Scientific Instruments*, 77 (8).

[28] Hrabina, J., Lazar, J., Klapetek, P., Cip, O. (2011). Multidimensional interferometric tool for the local probe microscopy nanometrology. *Measurement Science & Technology*, 22 (9).

[29] Cao, H.J., Zang, E.J., Zhao, K., Zhang, X.B., Wu, Y.X., Shen, N.C. (1998). Frequency stabilization of a Nd:YAG laser to Doppler-broadened lines of iodine near 532 nm. In *Conference on Precision Electromagnetic Measurements Digest*, 6-10 July 1998. IEEE, 183-184.

[30] Lazar, J., Hrabina, J., Sery, M., Klapetek, P., Cip, O. (2012). Multiaxis interferometric displacement measurement for local probe microscopy. *Central European Journal of Physics*, 10 (1), 225-231.

[31] du Burck, F., Daussy, C., Amy-Klein, A., Goncharov, A.N., Lopez, O., Chardonnet, C., Wallerand, J.P. (2005). Frequency measurement of an Ar+ laser stabilized on narrow lines of molecular iodine at 501.7 nm. *IEEE Transactions on Instrumentation and Measurement*, 54 (2), 754-758.

[32] Wallerand, J.P., Robertsson, L., Ma, L.S., Zucco, M. (2006). Absolute frequency measurement of molecular iodine lines at 514.7 nm, interrogated by a frequency-doubled Yb-doped fibre laser. *Metrologia*, 43 (3), 294-298.

[33] Osellame, R., Della Valle, G., Chiodo, N., Taccheo, S., Laporta, P., Svelto, O., Cerullo, G. (2008). Lasing in femtosecond laser written optical waveguides. *Applied Physics A : Materials Science & Processing*, 93 (1), 17-26.

[34] Chiodo, N., Du Burck, F., Hrabina, J., Candela, Y., Wallerand, J.P., Acef, O. (2013). CW frequency doubling of 1029 nm radiation using single pass bulk and waveguide PPLN crystals. *Optics Communications,* 311, 239-244.

[35] Chiodo, N., Du-Burck, F., Hrabina, J., Lours, M., Chea, E., Acef, O. (2014). Optical phase locking of two infrared continuous wave lasers separated by 100 THz. *Optics Letters*, 39 (10), 2936-2939.

[36] Hrabina, J., Jedlicka, P., Lazar, J. (2008). Methods for measurement and verification of purity of iodine cells for laser frequency stabilization. *Measurement Science Review*, 8 (5), 118-121.

[37] Fang, H.M., Wang, S.C., Liu, L.C., Cheng, W.Y., Wu, K.Y., Shy, J.T. (2006). Measurement of hyperfine splitting of molecular iodine at 532 nm by double-passed acousto optic modulator frequency shifter. *Japanese Journal of Applied Physics*, 45, 2776-2779.

[38] Vigue, J., Broyer, M., Lehmann, J.C. (1981). Natural hyperfine and magnetic predissociation of the I_2 B state. I. - Theory. *Journal de Physique*, 42 (7), 937-947.

[39] Vigue, J., Broyer, M., Lehmann, J.C. (1981). Natural hyperfine and magnetic predissociation of the I_2 B state. II. - Experiments on natural and hyperfine predissociation. *Journal de Physique*, 42 (7), 949-959.

[40] Vigue, J., Broyer, M., Lehmann, J.C. (1981). Natural hyperfine and magnetic predissociation of the I_2 B state. III. - Experiments on magnetic predissociation. *Journal de Physique*, 42 (7), 961-978.

[41] Pique, J.P., Bacis, R., Hartmann, F., Sadeghi, N., Churassy, S. (1983). Hyperfine predissociation in the B state of iodine investigated through lifetime measurements of individual hyperfine sublevels. *Journal de Physique*, 44 (3), 347-351.

Received August 27, 2013.
Accepted July 25, 2014.